

# Changes in the mechanical properties of bioactive borophosphate fiber when immersed in aqueous solutions

Ayush Mishra, Panu Noppari, Catherine Boussard-Plédel, Laetitia Petit,  
Jonathan Massera

► **To cite this version:**

Ayush Mishra, Panu Noppari, Catherine Boussard-Plédel, Laetitia Petit, Jonathan Massera. Changes in the mechanical properties of bioactive borophosphate fiber when immersed in aqueous solutions. International Journal of Applied Glass Science, Wiley, In press, 10.1111/ijag.15514 . hal-02797041

HAL Id: hal-02797041

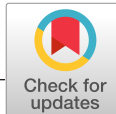
<https://hal-univ-rennes1.archives-ouvertes.fr/hal-02797041>

Submitted on 5 Jun 2020

**HAL** is a multi-disciplinary open access archive for the deposit and dissemination of scientific research documents, whether they are published or not. The documents may come from teaching and research institutions in France or abroad, or from public or private research centers.

L'archive ouverte pluridisciplinaire **HAL**, est destinée au dépôt et à la diffusion de documents scientifiques de niveau recherche, publiés ou non, émanant des établissements d'enseignement et de recherche français ou étrangers, des laboratoires publics ou privés.





# Changes in the mechanical properties of bioactive borophosphate fiber when immersed in aqueous solutions

Ayush Mishra<sup>1</sup> | Panu Noppari<sup>1</sup> | Catherine Boussard-Plédel<sup>2</sup> | Laetitia Petit<sup>1,3</sup> | Jonathan Massera<sup>1</sup>

<sup>1</sup>Faculty of Medicine and Health Technology, Tampere University, Tampere, Finland

<sup>2</sup>Equipe Verres et Céramiques, UMR-CNRS 6226, Institut des Sciences Chimiques de Rennes, Université de Rennes I, Rennes Cedex, France

<sup>3</sup>Photonics Laboratory, Tampere University, Tampere, Finland

## Correspondence

Jonathan Massera, Faculty of Medicine and Health Technology, Tampere University, Korkeakoulunkatu 3, FI-33720 Tampere, Finland.

Email: jonathan.massera@tuni.fi

## Funding information

Academy of Finland, Grant/Award Number: 275427; Initial Funding For Research Costs, Grant/Award Number: 284492; Flagship Programme, Photonics Research and Innovation, Grant/Award Number: PREIN-320165; Academy Project, Grant/Award Number: 308558

## Abstract

Bioactive fibers have become increasingly prevalent for applications in optical sensing and as reinforcement in fully biodegradable devices. However, the typical bioactive glass fibers drawn from silicate glasses have poor mechanical properties. Here, we present our latest study on the development of new bioactive single-core (SC) borophosphate fiber with the composition (in mol%) 47.5P<sub>2</sub>O<sub>5</sub>-20CaO-20SrO-10Na<sub>2</sub>O-2.5B<sub>2</sub>O<sub>3</sub> and of core-clad (CC) borophosphate fiber, the composition (in mol%) of the clad and the core being 47.5P<sub>2</sub>O<sub>5</sub>-20CaO-20SrO-10Na<sub>2</sub>O-2.5B<sub>2</sub>O<sub>3</sub> and 0.025CeO<sub>2</sub>-0.975(47.5P<sub>2</sub>O<sub>5</sub>-20CaO-20SrO-10Na<sub>2</sub>O-2.5B<sub>2</sub>O<sub>3</sub>), respectively. We show that the immersion in aqueous solutions such as Tris(hydroxymethyl)aminomethane (TRIS) increases first the mechanical properties of the fibers due to the early congruent glass dissolution and so due to the reduction in the density of surface flaws. However, for long immersion in TRIS or in Simulated Body Fluid (SBF), the mechanical properties decrease due to the precipitation of a reactive calcium-phosphate layer at the surface of the fibers. Especially when immersed for a long time in SBF, the fibers become too fragile to allow one to measure their mechanical properties. Nonetheless, we clearly show in this study that the newly developed fibers are promising materials for reinforcing composite and/or as biosensors as these fibers still possess sufficiently high mechanical properties after immersion for significant time in SBF and/or TRIS.

## KEYWORDS

durability, fibers, glass forming systems, glass manufacturing, mechanical properties, phosphate, surfaces

## 1 | INTRODUCTION

The use of glass fibers in modern health care has expanded from the use of chemically stable fiber, such as E-glass, commonly used as reinforcing agent in composites,<sup>1</sup> to the use of optical fiber for biosensing.<sup>2,3</sup> However, the common features

of the majority of the fibers used nowadays are their high SiO<sub>2</sub> content and/or the presence of toxic compound which prevents their clinical use. Indeed, the E-glass-based fibers or the fibers presented in the review by Bosch et al<sup>4</sup> have high silica content, leading to long-term stability in physiological media. Nearly inert glass fiber used for in vivo sensing or

This is an open access article under the terms of the Creative Commons Attribution License, which permits use, distribution and reproduction in any medium, provided the original work is properly cited.

© 2020 The Authors. *International Journal of Applied Glass Science* published by American Ceramics Society (ACERS) and Wiley Periodicals LLC

reinforcement would require an additional surgery to remove the fibers post-treatment before it becomes encapsulated by a fibrous tissue.<sup>5</sup> Alternatively, the chalcogenide glass family (containing elements such as Se, As, Ge, etc...) is used for biosensing to probe signals that are in the mid- and far-IR region.<sup>6</sup> However, these fibers can only be used *ex vivo* due to the presence of toxic elements. These fibers cannot be used for polymer reinforcement, for example.

In order to move toward fully resorbable biomaterials-based sensors or reinforcing agent, new bioactive/bioresorbable fibers should be developed to avoid additional manipulation of the patient to remove the biosensor after use.

The two main FDA (Food and Drug Administration) approved and used bioactive glasses are BonAlive<sup>®</sup> S53P4 and Bioglass<sup>®</sup> 45S5.<sup>7,8</sup> These bioactive glasses are silicate-based glasses with a SiO<sub>2</sub> content less than 60 mol%. Their structure is highly distorted, leading to crystallization upon heating or cooling as explained in reference 9. Therefore, drawing fibers from these bioactive glasses is challenging. Although De Diego et al succeeded in drawing fibers from Bioglass<sup>®</sup> 45S5, the fibers exhibited weak mechanical properties (93 MPa tensile strength) and high probability of premature failure (Weibull modulus  $m = 3$ ) limiting their clinical use.<sup>10</sup> Pirhonen et al and Clupper et al drew modified silicate-based bioactive glasses into fibers from 13-93 (a FDA-approved glass composition developed by Brink et al<sup>11</sup>), 9-93,<sup>12,13</sup> and S520.<sup>14</sup> These glasses differ from the typically used bioactive glass S53P4 and 45S5, as they contain less CaO and Na<sub>2</sub>O. Additional oxides such as K<sub>2</sub>O, B<sub>2</sub>O<sub>3</sub>, and MgO are added in these glasses to enhance the hot working domain. Despite the improvement in the tensile strength, the Weibull modulus of these silica based fibers still remains very low (~3).

Phosphate glasses are also known as biomaterials<sup>15</sup> and can be easily drawn into fibers.<sup>16</sup> A large number of studies were reported on phosphate glasses and fibers for medical applications from invert phosphate glasses<sup>17,18</sup> that cannot be drawn into fibers to metaphosphate glasses/fibers.<sup>19</sup> Ahmed et al evidenced that the addition of boron oxide or iron oxide into the phosphate network can lead to fibers with higher tensile strength and Weibull modulus than the silica-based bioactive fibers.<sup>20-24</sup> With regards to application in biosensing, Sglavo et al developed calcium phosphate fibers and capillaries with tensile strength of 200-350 MPa and Weibull modulus ranging from 3 to 6.<sup>25</sup> However, despite the good knowledge of the dissolution mechanism and kinetics of phosphate glasses, the impact of the fiber dissolution on its mechanical properties has been poorly studied. Especially one should keep in mind that during the dissolution of phosphate bioactive glasses, a CaP reactive layer may form at the glass/fiber surface leading to change in the mechanical properties of the glass/fiber. Therefore, there is a crucial need to understand the impact of early dissolution of fibers and of

late deposition of reactive CaP layer at their surface on their mechanical properties when the fibers are meant to be used as either reinforcing fibers in composites or biosensors.

In this study, we selected the glass with the (47.5P<sub>2</sub>O<sub>5</sub>-20CaO-20SrO-10Na<sub>2</sub>O-2.5B<sub>2</sub>O<sub>3</sub>) composition (in mol%) to be drawn into single-core (SC) and core-clad (CC) fibers to be used for example for reinforcement for polymer matrices. This glass system is promising for medical applications based on its glass *in vitro* dissolution properties, as reported in references 26,27. Here, we investigate the mechanical stability of the fibers during long-term storage in different aqueous solutions such as TRIS (Tris(hydroxymethyl)aminomethane) and SBF (simulated body fluid) in order to demonstrate that the developed fibers still possess sufficient mechanical properties after long immersion in these solutions. The mechanical properties of the fibers are discussed based on their tensile strength, Young's modulus, and Weibull modulus.

## 2 | EXPERIMENTAL PROCEDURE

The glass with composition (47.5P<sub>2</sub>O<sub>5</sub>-20CaO-20SrO-10Na<sub>2</sub>O-2.5B<sub>2</sub>O<sub>3</sub>) (in mol%) was used to produce the SC preform and also the clad of the CC preform. The composition of the core of the CC fiber was (0.025CeO<sub>2</sub>-0.975 (47.5P<sub>2</sub>O<sub>5</sub>-20CaO-20SrO-10Na<sub>2</sub>O-2.5B<sub>2</sub>O<sub>3</sub>) (in mol%). CeO<sub>2</sub> was added into the core composition in order to create a refractive index step between the core and the clad. The glasses were prepared by standard melting method using platinum crucible. NaPO<sub>3</sub>, H<sub>3</sub>BO<sub>3</sub>, and CeO<sub>2</sub> (all analytical grade) were used as raw materials. CaCO<sub>3</sub>, SrCO<sub>3</sub>, and NH<sub>4</sub>H<sub>2</sub>PO<sub>4</sub> (all analytical grade) were used to prepare Ca(PO<sub>3</sub>)<sub>2</sub> and Sr(PO<sub>3</sub>)<sub>2</sub>. Batches of 40 g of the glasses were melted at 1200°C for 1 hour. Ten-cm-long SC preforms with a diameter of 1 cm were obtained by casting the molten batches into a brass mold. The 10-cm-long CC preform with a diameter of 1 cm was obtained using the rotational casting method as in reference 28. Briefly, the clad composition was melted and poured into a preheated mold fixed into the rotational caster. The mold was then spun at 1000 rpm for 30 seconds to form a tube. Successively, the melt with core composition was poured into the hollow cladding. After quenching, the resulting CC rod was annealed at 400°C for 10 hours to remove the residual stress from the quenching.

Single-core fiber with 125 and 250 μm in diameter and CC step index fibers (75-125 and 150-250 μm in core and clad diameter, respectively) were drawn from preforms with a specially designed drawing tower as described in reference 26. The drawing temperature was 645°C for all the fibers. 40 m of uncoated fiber were drawn without any protective polymer layer to allow the measurement of the mechanical, structural, and *in vitro* dissolution properties.

Ten SC and CC fibers with a length of 15 cm were immersed in 12 mL of Tris(hydroxymethyl)aminomethane

(TRIS buffer solution) and Simulated Body Fluid (SBF) for at least 21 days at 37°C. The TRIS and SBF solutions were prepared as suggested by Sigma-Aldrich [Sigma-Aldrich Technical Bulletin No. 106B] and<sup>29</sup> respectively.

The pH of the fiber containing TRIS and SBF solutions was recorded over time using a Mettler Toledo SevenMulti™ pH/conductivity meter with an accuracy of  $\pm 0.02$  and compared to a blank solution containing only TRIS or SBF. The initial pH of TRIS and SBF solutions was 7.36 and 7.4, respectively, at 37°C.

The mechanical properties of the fibers were measured in tension and as a function of immersion time in TRIS and SBF using an Instron 4411 universal materials testing equipment. Postimmersion, the fibers were rinsed with ethanol and let to dry in a laminar hood, overnight, prior to testing. The grips were covered with a rubber mat to avoid the slipping of the fiber during the test and damaging the fiber with the metallic grips. A 500 N load cell was used, the grip distance was 50 mm, and the crosshead speed was set to 10 mm/min. The diameter of the fiber was measured using an optical microscope using a 20× magnification and the values for tensile strength and Young's modulus were calculated from the load-displacement curve. Displacement was determined by the machine cross-head motion. The stress was calculated as the  $F/A$ , where  $F$  is the force and  $A$  the nominal cross-section (measured for each fiber). The strain was calculated as  $\Delta L/L_0$ , where  $\Delta L$  is the change in gauge length and  $L_0$  the original gauge length. Prior to testing the newly developed fibers, the Instron equipment was tested using fibers with known mechanical properties under similar testing condition. The tensile strength and Young's modulus are reported as the mean and standard deviation of 10 measurements. The Weibull modulus was estimated as reported in references 12,13. However, it should be noted that the number of samples is low and values should be considered with care [ASTM C1239-13(2018)].

The Ca concentration in the solutions was quantified with an accuracy of  $\pm 15\%$  using an Atomic Absorption Spectrophotometer (AAS, AAnalyst 300; Perkin Elmer).

The IR absorption spectra of the glasses were recorded using Fourier transform infra-red spectroscopy (FTIR, Perkin Elmer) in attenuated total reflectance (ATR) mode on powdered glasses. All spectra were recorded within the 650-1600  $\text{cm}^{-1}$  range, corrected for Fresnel losses, and normalized to the absorption band showing the maximum intensity.

A scanning electron microscope (Carl Zeiss Crossbeam 540) equipped with Oxford Instruments X-Max<sup>N</sup> 80 EDS detector was used to image and analyze the samples. The samples were coated with a thin carbon layer.

### 3 | RESULTS

In this study, we selected the (47.5P<sub>2</sub>O<sub>5</sub>-20CaO-20SrO-10Na<sub>2</sub>O-2.5B<sub>2</sub>O<sub>3</sub>) composition (in mol%) due to its good

**TABLE 1** Tensile strength, Young's modulus, and Weibull modulus of the as-prepared fibers and of other fibers reported in literature

	Tensile strength (MPa)	Young's modulus (GPa)	Weibull modulus
SC			
125 $\mu\text{m}$	566 $\pm$ 83	63.8 $\pm$ 5.0	7.2 $\pm$ 0.3
250 $\mu\text{m}$	316 $\pm$ 40	31.0 $\pm$ 2.7	8.1 $\pm$ 0.4
CC			
125 $\mu\text{m}$	524 $\pm$ 102	71.9 $\pm$ 6.9	4.8 $\pm$ 0.3
250 $\mu\text{m}$	266 $\pm$ 53	34.1 $\pm$ 3.6	5.0 $\pm$ 0.4
45S5 [7]	93 $\pm$ 38		3.0
9-93 [8]	617 $\pm$ 292		2
13-93 [9]	441 $\pm$ 151		3
S520 [10]	925 $\pm$ 424		2.5

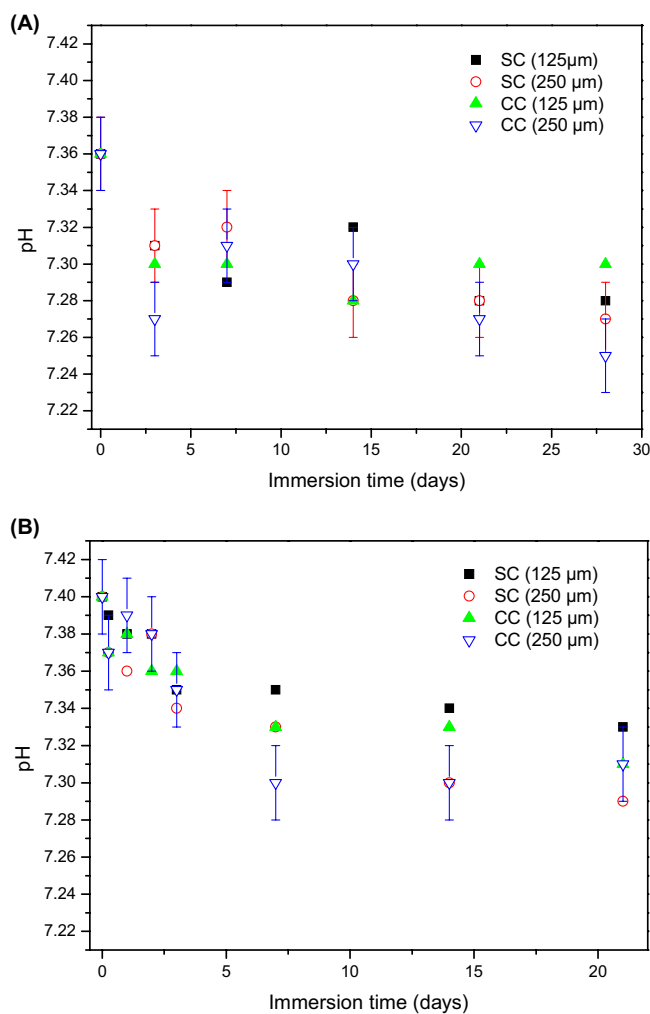


**FIGURE 1** pH of the Tris(hydroxymethyl)aminomethane buffer (A) and of the simulated body fluid (B) solutions containing the SC (single-core) and CC (core-clad) fibers with diameter 125 and 250  $\mu\text{m}$ , as a function of immersion time

bioactivity and fiber drawing capability as reported in reference 26. Single-core (labeled SC) and core-clad (labeled CC) fibers were drawn from this glass composition with a 125 and 250  $\mu\text{m}$  diameter. The mechanical properties of the fibers are reported in Table 1. The tensile strength and the Young's modulus decrease, whereas the Weibull modulus remains constant as the diameter of the (SC and CC) fibers increases from 125 to 250  $\mu\text{m}$ . The SC and CC fibers exhibit similar mechanical properties within the accuracy of the measurement, except for the Weibull modulus, which is larger for the SC fibers. After drawing, the fibers were immersed in TRIS and SBF for up to 21 days.

### 3.1 | Immersion in TRIS and SBF

The pH of the TRIS buffer solution and SBF was measured as a function of immersion time and is reported in Figure 1A,B, respectively. With an increase in the immersion time and regardless of the fibers design (SC vs CC), geometry (125 vs 250  $\mu\text{m}$ ), or immersion solution, the pH decreases. Whereas the pH of the TRIS buffer solution decreases slightly and progressively over time (Figure 1A), the decrease in the pH of the SBF solution (Figure 1B) is fast during the first 7 days of immersion and then remains constant within the error of the measurements for longer immersion.

Figure 2 presents the Ca concentration in the TRIS buffer solution (a) and in SBF (b) as a function of immersion time. The Ca concentration increases in all the TRIS solutions during the first 7-14 days of immersion and then remains constant for longer immersion (Figure 2A). No noticeable impact of the fiber design and geometry on the Ca release into the TRIS buffer solution can be seen. While the Ca concentration increases in TRIS buffer solution with an increase in immersion time (Figure 2A), a decrease in the Ca concentration in the SBF solution is clearly observed over time (Figure 2B). Such decrease in the Ca concentration is a sign of Ca consumption from the solution. Whereas the Ca consumption was found similar when immersing the 125 and 250  $\mu\text{m}$  fiber in SBF solution, a larger Ca consumption is observed in the solutions containing the SC fibers than in the solutions containing the CC fibers.

Figure 3A,B exhibit the tensile strength and Young's modulus of the (SC and CC) fibers after immersion in TRIS solution, respectively. Within the accuracy of measurement, the CC fibers exhibit a slight increase in the tensile strength and Young's modulus after 7-14 days in TRIS solution while an increase in the mechanical properties of the SC fibers is observed after 21 days in TRIS solution. The changes in these mechanical properties are more noticeable in the 125  $\mu\text{m}$  fibers compared to the 250  $\mu\text{m}$  fibers. Figure 3C,D exhibit the tensile strength and Young's modulus, respectively, of the (SC and CC) fibers after immersion in SBF. For all fibers

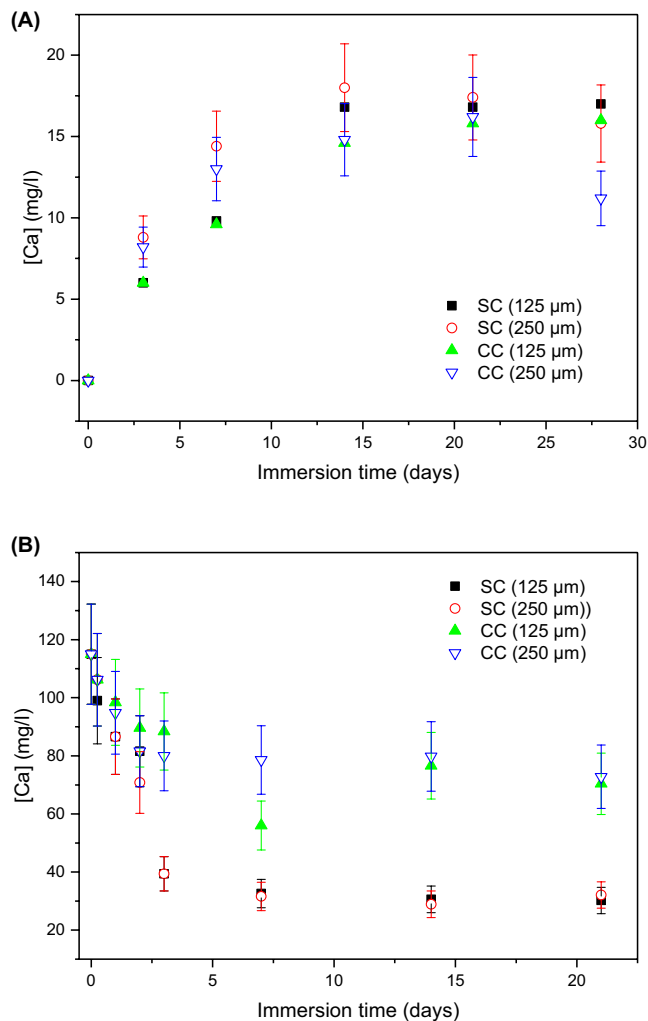


**FIGURE 2** Ca concentration in Tris(hydroxymethyl) aminomethane buffer solution (A) and simulated body fluid (B) solutions containing the SC (single-core) and CC (core-clad) fibers with diameter 125 and 250  $\mu\text{m}$ , as a function of immersion time

regardless of their design and diameter, the tensile strength and the Young's modulus of the SC fibers remain constant during the first  $\sim 7$  days of immersions and then decrease for longer immersion. The Young's modulus of the CC fibers remains constant for 7 days while their tensile strength starts to decrease after  $\sim 2$ -3 days of immersion. Note that at days 14 and 21, the CC fibers were brittle. They broke before performing the mechanical measurements, hence the lack of data in Figure 3C,D. For the fibers which could still be measured, their mechanical properties are given with a large error bars due to the difficulties in handling the brittle fibers.

Figure 4 exhibits the IR spectra of the SC (250  $\mu\text{m}$ ) fiber after immersion in SBF solution, taken as an example. All spectra were normalized to the band located at  $\sim 890$   $\text{cm}^{-1}$ . The spectra exhibit five absorption bands located around 1250, 1085, 890, 760, and 718  $\text{cm}^{-1}$  and two shoulders at  $\sim 1150$  and 990  $\text{cm}^{-1}$ . As explained in reference 30, the bands

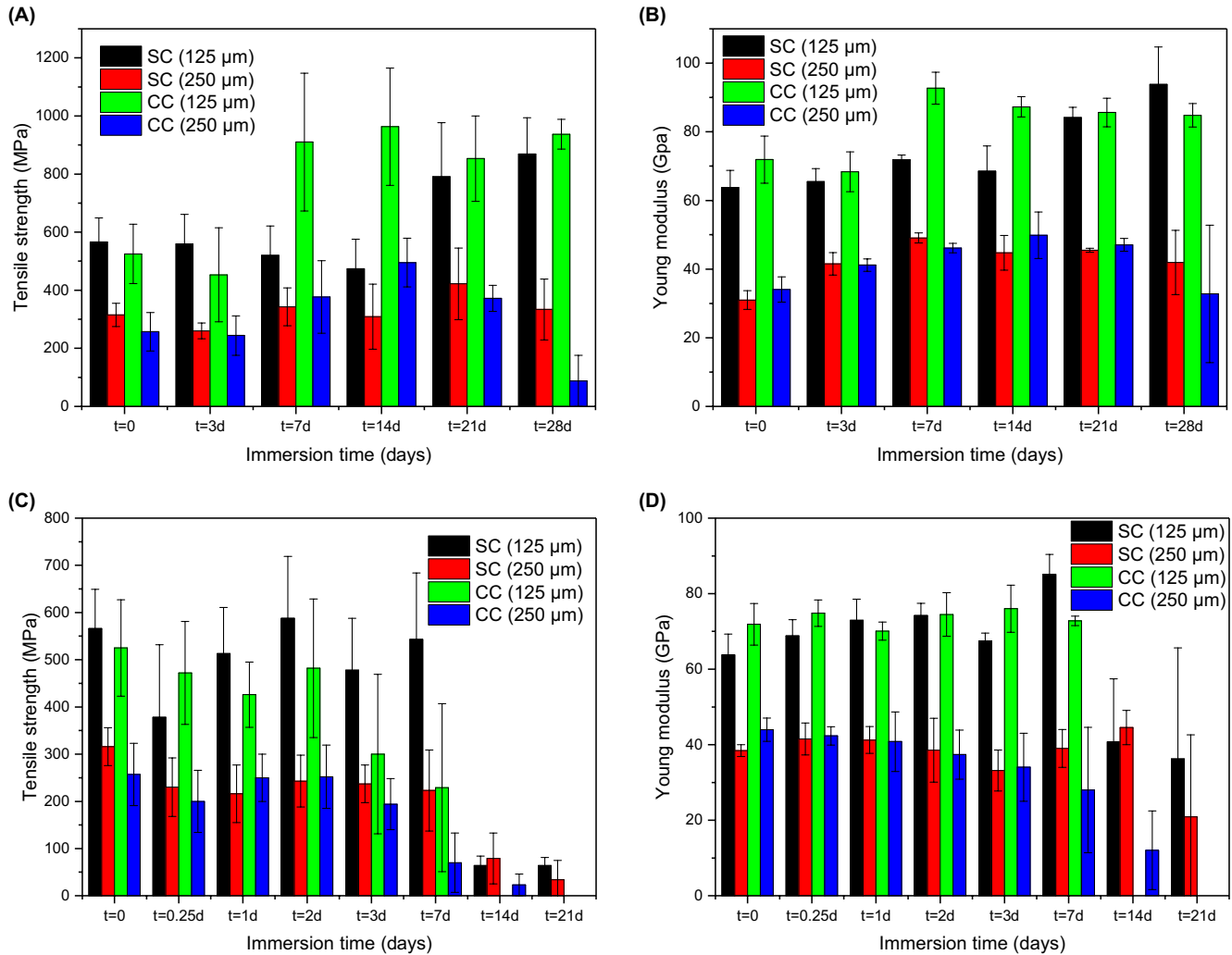


**FIGURE 3** Tensile strength and Young's modulus of the SC (single-core) and CC (core-clad) (125 and 250 μm) fibers as a function of immersion time in Tris(hydroxymethyl)aminomethane buffer solution (A, B) and in simulated body fluid (C, D), respectively

between 1150 and 1400  $\text{cm}^{-1}$  are characteristic of vibration of nonbridging  $\text{PO}_2$  groups. The band at 1250  $\text{cm}^{-1}$  can be assigned to asymmetric stretching modes,  $\nu_{\text{as}}(\text{PO}_2)$ , of the two nonbridging oxygen atoms bonded to a phosphorus atom in a  $\text{Q}^2$  phosphate tetrahedron and  $\text{BO}_4$  units.<sup>30-32</sup> The shoulder at 1150  $\text{cm}^{-1}$  corresponds to symmetric vibration of  $\text{PO}_2^{2-}$  in  $\text{Q}^2$  units. The bands in the 900-1150  $\text{cm}^{-1}$  range are characteristic of terminal P-O and  $\text{PO}_3$  groups. The shoulder centered at  $\sim 990 \text{ cm}^{-1}$  and the band at 1085  $\text{cm}^{-1}$  correspond to the symmetric and asymmetric stretching vibration of  $\text{PO}_3^{2-}$  in  $\text{Q}^1$  units, respectively.<sup>33,34</sup> The shoulder at 990  $\text{cm}^{-1}$  can also be attributed to the asymmetric stretching of the  $\text{BO}_4^-$  tetrahedra.<sup>35</sup> The band at 1085  $\text{cm}^{-1}$  can be also attributed to an overlap between  $\text{PO}_3 \text{ Q}^1$  terminal group and  $\text{PO}_2 \text{ Q}^2$  groups in metaphosphate.<sup>36</sup> The absorption bands located at 718 and 760  $\text{cm}^{-1}$  are characteristic of P-O-P symmetric stretching vibration in metaphosphate structure<sup>36</sup> and the band at 760 can be assigned to B-O-B bonds.<sup>35</sup> The main band at  $\sim 880 \text{ cm}^{-1}$  is attributed to P-O-P asymmetric stretching of bridging oxygen

in  $\text{Q}^2$  units ( $\nu_{\text{as}} \text{ P-O-P Q}^2$ ).<sup>29,37,38</sup> During the first 3 days in SBF solution, the fibers exhibit similar IR spectrum than the as-drawn fibers. However, for longer immersion in SBF solution, the band at 1250  $\text{cm}^{-1}$  decreases in intensity, whereas the band at 1085  $\text{cm}^{-1}$  increases in intensity as compared to the main band at 880  $\text{cm}^{-1}$ . The shoulder at 980  $\text{cm}^{-1}$  disappears while a new band at  $\sim 1017 \text{ cm}^{-1}$  appears in the spectra of the fibers immersed for more than 14 days.

## 4 | DISCUSSION

Bioactive glass fibers are of tremendous interest for composite reinforcement and/or for tissue engineering.<sup>14,39</sup> However, commercially used silicate bioactive glasses are prone to crystallization limiting their drawability.<sup>9</sup> Additionally, these glasses do not degrade fully in vivo leading to glass reminiscence even 14 years postoperation as reported in reference 40. Therefore, phosphate fibers have attracted much interest

due to their wider processing window and their promising biocompatibility.

Here, we investigate the changes in the mechanical properties of borophosphate fibers when immersed in TRIS buffer and SBF solutions to check if these fibers maintain sufficient mechanical properties upon immersion and so to check if they can be used for sensing, reinforcing of composite and/or as materials for tissue engineering scaffolds processing.

Single-core and CC fibers were successfully drawn from preforms. As seen in Table 1, the tensile strength and Young's modulus are independent of the design (SC vs CC) of the fiber, whereas both parameters decrease with increasing the fiber diameter. With increasing the fiber diameter, the density and distribution of critical sized flaws are suspected to increase and so are expected to reduce the tensile strength of the fibers as reported in reference 41. Additionally, the SC fibers exhibit a Weibull modulus of 7-8, whereas the Weibull modulus for the CC fibers is slightly lower ( $m=5$ ). This difference in the Weibull modulus could be related to a large stress and defect density at the interface between the core and the cladding as suggested in reference 42. The Young's modulus, however, is generally assumed to be independent of the fiber diameter. Only in the case of significant increase

in anisotropy, an increase in  $E$  is suspected to occur when the diameter of metaphosphate fibers decreases.<sup>43,44</sup> While, the tensile strength and Young's modulus of the investigated fibers are similar to those reported for other bioactive phosphate glass fibers, while having a larger diameter,<sup>18,22-24,45</sup> the change in the Young's modulus with decreasing the fiber diameter cannot, at present, be explained. Possible assumptions include (a) the slipping of the large fibers in the grip which would lead to an underestimation of the Young's modulus and/or (b) the aging (and water retention) of the fibers. Of course, those are sole assumptions and will be studied in future.

As the fibers are aimed to be used as scaffold materials in tissue engineering and/or in fiber reinforced composite, it is important to investigate the changes in their mechanical stability when immersed in various physiological media such as TRIS buffer and SBF solutions. The SC and CC fibers were immersed in those solutions for up to 21-28 days.

The decrease in the pH of both solutions over time seen in Figure 1 can be related to the release of phosphate from the glass to the solution as reported in reference 19. The slight decrease in the pH of both solutions (Figure 1) can be associated with the changes in the Ca content overtime (Figure 2) and so is a clear sign of the glass dissolution, which is expected to be congruent as suggested in references 19,46. Furthermore, the change in the diameter of the fibers is reported in Table 2, for immersion in TRIS buffer solution, taken as an example. One can clearly see the decrease in the diameter with increasing immersion time.

As seen in Figure 2, the Ca concentration increases and saturates after 14 days in TRIS buffer solution. Therefore, the calcium phosphate (CaP) layer is expected to start to precipitate at the surface of the fiber after ~14 days in this solution. The drop in the pH of the SBF solution (Figure 1B) and in the Ca concentration (Figure 2B) occurring already after 7 days indicates that this CaP layer precipitates faster at the surface of the fiber when immersing the fiber in the SBF solution than in the TRIS buffer solution. It should be noted that the TRIS buffer solution does not contain any alkali or alkaline earth ions,<sup>47</sup> whereas the SBF solution contains similar ion concentration than in the blood plasma and is supersaturated

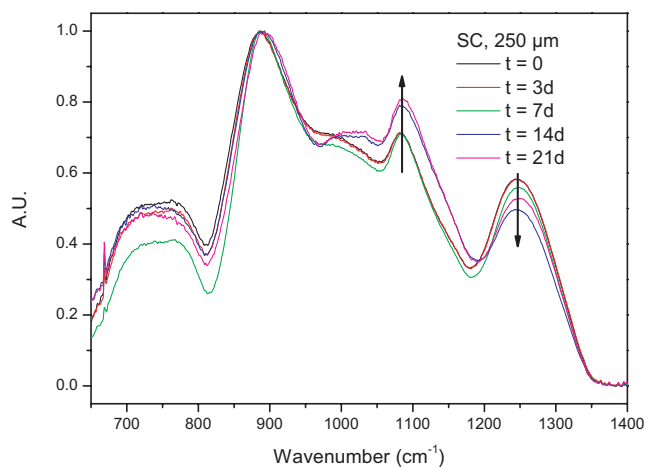


**FIGURE 4** IR spectra of the single-core (SC) fiber with a diameter 250μm immersed in simulated body fluid solution for up to 21 d

**TABLE 2** Fibers diameter as a function of immersion time in TRIS buffer solution (average of 10 fibers)

	Initial diameter (μm)	Average diameter at 3 d	Average diameter at 7 d	Average diameter at 14 d	Average diameter at 21 d	Average diameter at 28 d
SC						
	125 μm	123 ± 10	95 ± 14	85 ± 19	77 ± 12	69 ± 13
	250 μm	245 ± 14	215 ± 20	205 ± 11	192 ± 11	17 ± 13
CC						
	125 μm	128 ± 12	99 ± 10	82 ± 12	7 ± 6	65 ± 18
	250 μm	247 ± 19	221 ± 12	200 ± 18	185 ± 8	17 ± 15

toward precipitation of apatite crystals.<sup>48</sup> Therefore, it is the difference in the composition of the TRIS buffer and SBF solutions which leads to a slower precipitation of the CaP layer at the surface of the fiber when immersed in TRIS buffer solution than in the SBF solution. It is the progressive precipitation of the CaP layer at the surface of the fibers immersed in both solutions which is thought to decrease their mechanical properties shown in Figure 3.

The initial increase in the tensile strength seen in Figure 3A,B after immersing the fibers in TRIS solution can be related to the congruent glass dissolution which decreases the number of the surface defects such as flaws. However, a change in the density of surface critical flaws is not sufficient to explain the slight increase in the Young's modulus seen in Figure 3. Indeed the Young modulus is a bulk property, independent of surface defects. Therefore, as it was demonstrated in reference 16, a possible explanation of the slight increase in the Young's modulus could come from the migration of Na at the surface of the fiber occurring during the fiberization process, and the subsequent depletion of Na away from the surface. This could lead to a gradient of structural properties across the diameter of the fiber which may lead to variation in mechanical properties. However, one should repeat the measurement on a greater number of fibers to ensure statistical differences. Therefore, it appears that in order to increase the mechanical properties of the fibers, a preincubation in an aqueous buffer solution would be beneficial. It should be noted that an increase in the tensile strength of the bioactive silica fiber 13-93 was observed upon immersion in the SBF solution<sup>13</sup> and was attributed to the formation of a SiO<sub>2</sub> gel which overcomes the presence of the flaws present at the fiber surface.<sup>13</sup> Here, the congruent dissolution of the investigated borophosphate fibers in SBF does not lead to the formation of a gel but to a rapid precipitation of the CaP layer at the surface of the fiber. Because the mechanical properties of the fibers remain constant for short immersion in the SBF solution (Figure 3C,D), the reactive CaP layer is suspected not to bond to the surface of the fiber, but rather to pill-off. Similar results were reported for bulk glasses with composition 50P<sub>2</sub>O<sub>5</sub>-(40-x)CaO-xSrO-10Na<sub>2</sub>O<sup>49</sup> and with fibers within

the metaphosphate composition.<sup>50</sup> However, for long immersion in SBF, the CaP layer is expected to bond to the surface of the fiber leading to a decrease in the mechanical properties of the fibers. The mechanical properties of the immersed fiber, especially the Young's modulus, do not anymore correspond to those of the glass fiber alone but to those of a combination of the glass coated with a weakly adherent ceramics layer.

The presence of the CaP layer at the surface of the fibers was confirmed using FTIR and SEM. Figure 4 exhibits the IR spectra measured at the surface of the SC (250 μm) fiber after immersion in the SBF solution. The IR spectra of the other fibers immersed in both solutions were analyzed and they all exhibit similar structural changes overtime. For short immersion (<3 days), no noticeable structural modifications occur confirming that the CaP layer is not bonded at the surface of the fiber. However, for longer immersion, a decrease in intensity of the band attributed to Q<sup>2</sup> units and an increase in intensity of the band related to Q<sup>1</sup> units are observed indicating that the P-O-P bonding are being broken which is a clear sign of initial glass dissolution. More importantly, the appearance of the band at 1017 cm<sup>-1</sup> is a clear sign of the precipitation of a CaP layer at the surface of the fibers in agreement with.<sup>16</sup> As this band is only visible in the spectrum of the fibers immersed in SBF for more than 14 days, we confirm that the CaP layer is bonded to the surface of the fibers only after 14 days in SBF in agreement with the changes in the pH solution (Figure 1B) and in the Ca concentration in the solution (Figure 2B). The formation of the CaP layer was confirmed using SEM coupled with EDS and was correlated with the steep decrease in the Young's modulus seen in Figure 3D. As depicted in Figure 5, the surface of the as-drawn SC fiber is smooth and free of large defects while a layer can be seen at the surface of the fibers after immersion in SBF and TRIS solutions. The layer appeared to have cracked and this is typically associated with the drying of the reactive layer. Additionally, from the EDX analysis, the as-drawn fibers exhibit a (Ca+Sr)/P ratio of (~0.37 ± 0.01), which is close to the 0.42 expected from the nominal composition. After 2 weeks of immersion in SBF, a significant increase in the Ca content and drop in the Sr and P contents were noticed. The (Ca+Sr)/P ratio was found to increase to (~0.57 ± 0.01). These

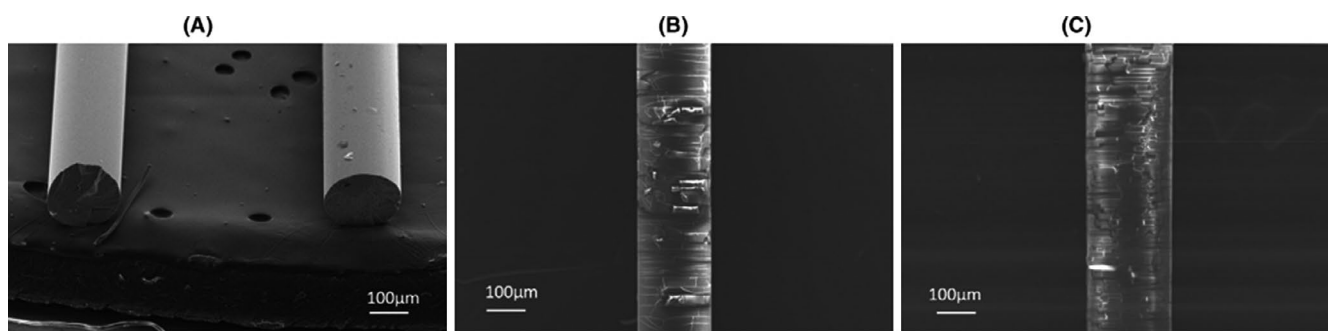


**FIGURE 5** SEM images of the single-core fiber (SC) prior to immersion (A) and after immersion for 2 wk in simulated body fluid solution (B) and 4 wk in Tris(hydroxymethyl)aminomethane buffer solution (C)



changes in the glass composition indicate that a Sr-substituted CaP layer is formed at the fiber surface. After 4 weeks in TRIS, the (Ca+Sr)/P ratio increases to ( $\sim 0.53 \pm 0.01$ ) which is slightly lower than the (Ca+Sr)/P ratio measured at the surface of the fiber immersed in SBF. This might be assigned to the layer being thinner upon immersion in TRIS than in SBF. Similar analysis was performed on the CC fibers leading to similar conclusions. Figure 6 shows the SEM image of a CC fiber immersed for 4 weeks in TRIS buffer solution. The fiber's cross-section that was exposed to the solution and not fractured during the mechanical test was imaged. One can clearly see the core and the clad. As seen for the SC fibers, a reactive layer is present at the surface of the CC fibers. It is interesting to note that the core started to degrade.

It should be pointed out that the changes in the pH of the TRIS and SBF solutions and in the Ca concentration in these solutions over time are independent of the fiber geometry and design within the accuracy of the measurement. This is due to the fact that the composition of the glass in contact with the solution is the same in the SC and CC fibers. However, different mechanical properties of the immersed fibers were measured depending on their geometries and designs; smaller increase in the mechanical properties of the (250  $\mu\text{m}$ ) fibers as compared to the (125  $\mu\text{m}$ ) fibers and faster increase in the mechanical properties of the CC fibers compared to that of the SC fibers were measured after immersion in both solutions. It is well known that the fiber strength is controlled by submicroscopic damage at the surface of the fibers.<sup>50-52</sup> The fibers with large diameter have large surface area and therefore are more likely to possess a defect with critical size that will govern the overall fibers' mechanical properties.<sup>9,53</sup> Despite the slightly faster dissolution rate with increasing the fibers surface area, it is conceivable that, even postimmersion, all flaws with critical size are not suppressed in the fiber with larger diameter.

The difference in the mechanical properties of the SC and the CC fibers might be due to the preform manufacturing process.

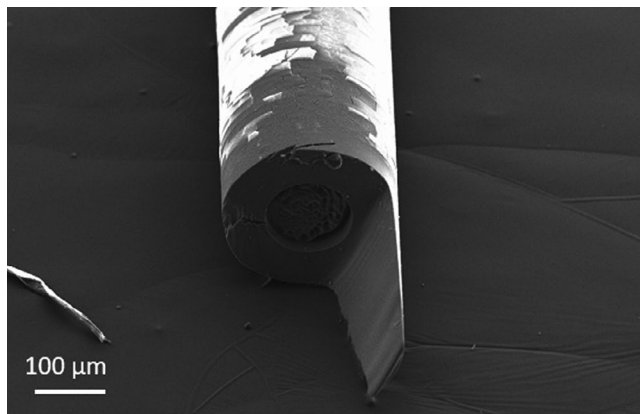


**FIGURE 6** SEM images of the core-clad fiber (CC) after immersion for 4 wk in Tris(hydroxymethyl)aminomethane buffer solution

Indeed, the fiber drawing process is also known to induce phosphate chain reorientation,<sup>16,54,55</sup> as well as migration of mobile ions to the fibers' surface.<sup>16,20</sup> It is therefore possible that the difference in the thermal history between the SC and CC fibers leads to some structural and compositional variations at the fibers surface. Indeed, when the CC preform is manufactured, the melt of the core composition is cast into the solidified cladding tube leading to second cycle of heating/cooling for the clad glass that might lead to further ion diffusion at the cladding surface. It is noteworthy that the rotational casting method is thought to lead to an optimum CC interface as already seen in reference 56.

Interestingly, the solutions which contain the fibers with larger diameter exhibit a slightly lower pH than the solutions with the fibers with smaller diameter for long-term immersion in both TRIS buffer and SBF solutions. This is especially true for the SC fibers. This might be attributed to the high surface of the large diameter fibers leading to slightly faster dissolution rate.

Surprisingly, as seen in Figure 2B, a larger concentration of Ca was detected in the solutions containing the CC fibers than in the solutions with the SC fibers indicating that the SC fibers consumed more Ca than the CC fibers. As the same glass composition is in contact with the SBF in both SC and CC fibers, an identical Ca consumption from the SC and CC fibers is expected. The differences in Ca consumption are not yet fully understood and more research on the surface chemistry of the CC and SC fibers is ongoing.

The as-drawn fibers of investigation possess a Young's modulus ranging from  $\sim 35$  to 60 GPa depending on the fiber dimension. The fibers were found to resorb in aqueous solution, producing a CaP layer indicating that these fibers will promote cell attachment and proliferation when implanted in the body.<sup>49</sup> The high Weibull modulus of these fibers compared to that of silicate fibers is also an advantage as the investigated fibers are less likely to undergo premature failure than silicate fibers. It is important to note that metals and alloys are typically used for internal fracture fixation. However, they need to be surgically removed after use. Additionally, the mismatch between the Young's modulus of the cortical bone (17-24 GPa) and of the metals or alloys (100-200 GPa) leads to high stress concentration at the bone/implant interface.<sup>57</sup> Polymer fixation had been developed in view of processing fully resorbable implant which will alleviate the need for the secondary surgery. However, although the mechanical properties of the resorbable polymers have been improved, these polymers still possess a low Young's modulus (typically  $< 10$  GPa<sup>58</sup>), which may lead to excessive bone motion, impeding proper bone healing. Therefore, the investigated fibers appear to be suitable materials for reinforcement of polymeric matrices and for the processing of fully resorbable composites for internal fracture fixation. Indeed their Young's modulus remains  $> 30$  GPa for fibers with a 250  $\mu\text{m}$  diameter and  $> 60$  GPa for fibers with a 125  $\mu\text{m}$  diameter until a thick reactive layer forms ( $\sim 7$ -14 days in SBF solution and  $\sim$  after 21 days

in the TRIS buffer solution) with thickness of ~1-5  $\mu\text{m}$ . Once incorporated in a polymeric matrix, one can expect that the mechanical properties will drop at even longer immersion time. Aside from their bioactive and mechanical properties, one should keep in mind that phosphate fibers were initially developed for laser applications,<sup>59</sup> and, therefore, these fibers could also find potential in application where the fibers would be used as biosensors.<sup>16,27</sup>

## 5 | CONCLUSION

In this study, borophosphate SC and CC fibers were drawn from preforms. Their mechanical properties (Tensile strength and Young's modulus) were measured upon immersion in the SBF and the TRIS buffer solutions. The initial congruent dissolution of the fibers enhances the mechanical properties of the fibers indicating that, prior to use the bioactive phosphate fiber as reinforcement, the fibers should be preincubated for few days in the TRIS buffer solution in order to reduce the amounts of flaws density at the surface of the fiber without forming a calcium phosphate layer and so to increase the fiber mechanical properties. Indeed, when immersed for longer time (~7-14 days in SBF solution and ~21 days in the TRIS buffer solution), a calcium phosphate layer starts to precipitate at the surface of the fibers reducing their mechanical properties.


We also show that CC fibers exhibit similar mechanical properties and slightly faster reaction rate than their SC counterpart fibers opening the path to the use of optical CC fibers with bioactive properties. Such fibers could find great interest for probing glass dissolution in vitro or in vivo.

## ACKNOWLEDGMENTS

The authors would like to acknowledge the financial support of the Academy of Finland through the Academy Research Fellow grant (275427), the Initial Funding For Research Costs (284492), Flagship Programme, Photonics Research and Innovation (PREIN-320165), and Academy Project (326418).

## ORCID

Laeticia Petit <http://orcid.org/0000-0002-1673-8996>

Jonathan Massera  <https://orcid.org/0000-0002-1099-8420>

## REFERENCES

- Zhang M, Matinlinna JP. E-glass fiber reinforced composites in dental applications. *Silicon*. 2012;4(1):73–8.
- Clupper DC, Hall MM, Gough JE, Hench LL. *Transactions of the Society for Biomaterials*. Tampa, FL, 2002.
- Baldini F, Giannetti A, Mencaglia AA, Trono C. Fiber optic sensors for biomedical applications. *Curr Anal Chem*. 2008;4(4):378–90.
- Bosch ME, Sanchez AJR, Rojas FS, Ojeda CB. Recent development in optical fiber biosensors. *Sensors*. 2007;7(6):797–859.
- Hench L, Best S. *Ceramics, glasses and glass-ceramics*. In: Rater B, Hoffman A, Schoen FJ, Lemons JE, editors. *Biomaterials science*. 2nd ed. San Diego: Elsevier; 2004.
- Anne M-L, Keirsse J, Nazabal V, Hyodo K, Inoue S, Boussard-Pledel C, et al. Chalcogenide glass optical waveguide for infrared biosensing. *Sensors*. 2009;9(9):7398–411.
- Andersson OH, Karlsson KH. *Corrosion of bioactive glass under various in vitro conditions*. *Advance in Biomaterials No 8*. Amsterdam: Elsevier; 1990.
- Hench LL, Andersson OH. *Bioactive glasses*. In: Wilson J, editor. *An introduction to bioceramics*. Singapore: World Scientific Publishing Co; 1993.
- Massera J, Fagerlund S, Hupa L, Hupa M. Crystallization mechanism of the bioactive glasses, 45S5 and S53P4. *J Am Ceram Soc*. 2012;95(2):607–13.
- De Diego MA, Coleman NJ, Hench LL. Tensile properties of bioactive fibers for tissue engineering applications. *J Biomed Mater Res B Appl Biomater*. 2000;53(3):199–203.
- Brink M. The influence of alkali and alkaline earths on the working range for bioactive glasses. *J Biomed Mater Res*. 1997;36(1):109–17.
- Pirhonen E, Moimas L, Brink M. Mechanical properties of bioactive glass 9–93 fibres. *Acta Biomater*. 2006;2(1):103–7.
- Pirhonen E, Niiranen H, Niemelä T, Brink M, Törmälä P. Manufacturing, mechanical characterization, and in vitro performance of bioactive glass 13–93 fibers. *J Biomed Mater Res B*. 2006;77(2):227–33.
- Clupper DC, Gough JE, Hall MM, Clare AG, LaCourse WC, Hench LL. In vitro bioactivity of S520 glass fibers and initial assessment of osteoblast attachment. *J Biomed Mater Res A*. 2003;67(1):285–94.
- Clement J, Manero JM, Planell JA. Analysis of the structural changes of a phosphate glass during its dissolution in simulated body fluid. *J Mater Sci Mater Med*. 1999;10(12):729–32.
- Massera J, Ahmed I, Petit L, Aallos V, Hupa L. Phosphate-based glass fiber vs. bulk glass: change in fiber optical response to probe in vitro glass reactivity. *Mater Sci Eng C*. 2014;37:251–7.
- Lee S, Obata A, Brauer DS, Kasuga T. Dissolution behavior and cell compatibility of alkali-free MgO-CaO-SrO-TiO<sub>2</sub>-P<sub>2</sub>O<sub>5</sub> glasses for biomedical applications. *Biomed Glas*. 2015;1:151–8.
- Islam MDT, Hossain KZ, Sharmin N, Parsons AJ, Ahmed I. Effect of magnesium content on bioactivity of near invert phosphate-based glasses. *Int J Appl Glass Sci*. 2017;8(4):391–402.
- Colquhoun R, Tanner KE. Mechanical behaviour of degradable phosphate glass fibres and composites – a review. *Biomed Mater*. 2015;11(1):014105.
- Sharmin N, Hasan MS, Parsons AJ, Rudd CD, Ahmed I. Cytocompatibility, mechanical and dissolution properties of high strength boron and iron oxide phosphate glass fibre reinforced bioresorbable composites. *J Mech Behav Biomed*. 2016;59:41–56.
- Sharmin N, Parsons AJ, Rudd CD, Ahmed I. Effect of boron oxide addition on fibre drawing, mechanical properties and dissolution behaviour of phosphate-based glass fibres with fixed 40, 45 and 50 mol% P<sub>2</sub>O<sub>5</sub>. *J Biomater Appl*. 2014;29(5):639–53.
- Haque P, Ahmed I, Parsons A, Felfel R, Walker G, Rudd RC. Degradation properties and microstructural analysis of 40P<sub>2</sub>O<sub>5</sub>–24MgO–16CaO–16Na<sub>2</sub>O–4Fe<sub>2</sub>O<sub>3</sub> phosphate glass fibres. *J Non-Cryst Solids*. 2013;375:99–109.
- Hasan MS, Ahmed I, Parsons A, Walker G, Scotchford C. Cytocompatibility and mechanical properties of short phosphate

- glass fibre reinforced polylactic acid (PLA) composites: effect of coupling agent mediated interface. *J Funct Biomater*. 2012;3(4):706–25.
24. Ahmed I, Parsons AJ, Palmer G, Knowles JC, Walker GS, Rudd CD. Weight loss, ion release and initial mechanical properties of a binary calcium phosphate glass fibre/PCL composite. *Acta Biomater*. 2008;4(5):1307–14.
  25. Sglavo V, Pugliese D, Sartori F, Boetti NG, Ceci-Ginestrelli E, Franco G, et al. Mechanical properties of resorbable calcium-phosphate glass optical fiber and capillaries. *J Alloys Compd*. 2019;778:410–7.
  26. Massera J, Shpotyuk Y, Sabatier F, Jouan T, Boussard-Plédel C, Roiland C, et al. Processing and characterization of novel borophosphate glasses and fibers for medical applications. *J Non-Cryst Solids*. 2015;425:52–60.
  27. Mishra A, Désévéday F, Smektala F, Massera J. Core-clad phosphate glass fibers for biosensing. *Mater Sci Eng C*. 2019;96:458–65.
  28. Massera J, Haldeman A, Milanese D, Gebavi H, Ferraris M, Foy P, et al. Processing and characterization of core-clad tellurite glass preforms and fibers fabricated by rotational casting. *Opt Mater*. 2010;32(5):582–8.
  29. Kokubo T, Kushitani H, Sakka S, Kitsugi T, Yamamuro T. Solutions able to reproduce in vivo surface-structure changes in bioactive glass-ceramic A-W<sup>3</sup>. *J Biomed Mater Res*. 1990;24(6):721–34.
  30. Carta D, Qiu D, Guerry P, Ahmed I, Neel EAA, Knowles JC, et al. The effect of composition on the structure of sodium borophosphate glasses. *J Non-Cryst Solids*. 2008;354(31):3671–7.
  31. Sharmin N, Hasan MS, Parsons AJ, Furniss D, Scotchford CA, Ahmed I, et al. Effect of boron addition on the thermal, degradation, and cytocompatibility properties of phosphate-based glasses. *Biomed Res Int*. 2013;2013:902427.
  32. Yao A, Rahaman MN, Lin J, Huang W. Structure and crystallization behavior of borate-based bioactive glass. *J Mater Sci*. 2007;42:9730–5.
  33. Gao H, Tan T, Wang D. Effect of composition on the release kinetics of phosphate controlled release glasses in aqueous medium. *J Control Release*. 2004;96(1):21–8.
  34. Abou Neel EA, Chrzanowski W, Pickup DM, O'Deel LA, Mordan NJ, Newport RJ, et al. Structure and properties of strontium-doped phosphate-based glasses. *J R Soc Interface*. 2009;6(34):435–46.
  35. Yiannopoulos YD, Chryssikos GD, Kamitsos EI. Structure and properties of alkaline earth borate glasses. *Phys Chem Glasses*. 2001;42(3):164–72.
  36. Ilieva D, Jivov B, Bogachev G, Petkov C, Penkov I, Dimitriev Y. Infrared and Raman spectra of Ga<sub>2</sub>O<sub>3</sub>-P<sub>2</sub>O<sub>5</sub> glasses. *J Non-Crystal Solids*. 2001;283(1–3):195–202.
  37. Shih P-Y, Shiu H-M. Properties and structural investigations of UV-transmitting vitreous strontium zinc metaphosphate. *Mater Chem Phys*. 2007;106(2–3):222–6.
  38. Moustafa YM, El-Egili K. Infrared spectra of sodium phosphate glasses. *J Non-Crystal Solids*. 1998;240(1–3):144–53.
  39. Jukola H, Nikkola L, Gomes E, Chiellini F, Tukiainen M, Kellomäki M, et al. Development of a bioactive glass fiber reinforced starch-polycaprolactone composite. *J Biomed Mater Res B*. 2008;87(1):197–203.
  40. Lindfors NC, Koski I, Heikkilä JT, Mattila K, Aho AJ. A prospective randomized 14-year follow-up study of bioactive glass and autogenous bone as bone graft substitutes in benign bone tumors. *J Biomed Mater Res B*. 2010;94(1):157–64.
  41. Ramsteiner F, Theysohn R. The influence of fibre diameter on the tensile behaviour of short-glass-fibre reinforced polymers. *Compos Sci Technol*. 1985;24(3):231–40.
  42. Ainslie BJ, Beales KJ, Cooper DM, Day CR, Rush JD. Drawing-dependent transmission loss in germania-doped silica optical fibres. *J Non-Crystal Solids*. 1982;47(2):243–5.
  43. Stockhorst H, Bruckner R. Structure sensitive measurements on phosphate glass fibers. *J Non-Crystal Solids*. 1986;85(1–2):105–26.
  44. Endo J, Inaba S, Ito S. Mechanical properties of anisotropic metaphosphate glasses. *J Am Ceram Soc*. 2015;98(9):2767–71.
  45. Cozien-Cazuc S, Parsons A, Walker GS, Jones IA, Rudd CD. Effects of aqueous aging on the mechanical properties of P<sub>40</sub>Na<sub>20</sub>Ca<sub>16</sub>Mg<sub>24</sub> phosphate glass fibres. *J Mater Sci*. 2008;43:4834–9.
  46. Bunker BC, Arnold GW, Wilder JA. Phosphate glass dissolution in aqueous solutions. *J Non-Crystal Solids*. 1984;64(3):291–316.
  47. Fagerlund S, Hupa L, Hupa M. Comparison of reactions of bioactive glasses in different aqueous solutions: in *Advances in Bioceramics and Biotechnologies* (Narayan R, McKittrick J, Singh M, editors). Hoboken, NJ: John Wiley and Sons Inc; 2010.
  48. Bohner M, Lemaître J. Can bioactivity be tested in vitro with SBF solution? *Biomaterials*. 2009;30(12):2175–9.
  49. Massera J, Kokkari A, Närhi T, Hupa L. The influence of SrO and CaO in silicate and phosphate bioactive glasses on human gingival fibroblasts. *J Mater Sci Mater Med*. 2015;26(6):196.
  50. Ahmed I, Shaharuddin SS, Sharmin N, Furniss D, Rudd C. Core/clad phosphate glass fibres containing iron and/or titanium. *Biomed Glas*. 2015;1:20–30.
  51. Kurkjian CR. Mechanical properties of phosphate glasses. *J Non-Crystal Solids*. 2000;263–264:207–12.
  52. Pukh V, Baikova L, Kireenko M, Tikhonova L. On the kinetics of crack growth in glass. *Glass Phys Chem*. 2009;35(6):560–6.
  53. Järvelä P. Properties of glass fibres and their applications in porous composites. Doctoral thesis. Tampere: Tampere University of Technology; 1983.
  54. Goldstein M, Davis TH. Glass fibers with oriented chain molecules. *J Am Chem Soc*. 1955;38(7):223–6.
  55. Milberg ME, Daly MC. Structure of oriented sodium metaphosphate glass fibers. *J Chem Phys*. 1963;39:2966–73.
  56. Mura E, Lousteau J, Milanese D, Abrate S, Sglavo VM. Phosphate glasses for optical fibers: synthesis, characterization and mechanical properties. *J Non-Crystal Solids*. 2013;362(1):147–51.
  57. Brauer DS, Rüssel C, Vogt S, Weisser J, Schnabelrauch M. Degradable phosphate glass fibers reinforced polymer matrices: mechanical properties and cell response. *J Mater Sci Mater Med*. 2008;19:121–7.
  58. Daniels AU, Chang MKO, Andriano KP, Heller J. Mechanical properties of biodegradable polymers and composites proposed for internal fixation of bone. *J Appl Biomater*. 1990;1(1):57–78.
  59. Schülzgen A, Li L, Zhu X, Albert J, Peyghambarian N. Recent Advances in Phosphate Glass Fiber Lasers, Conference on Lasers and Electro-Optics and 2009 Conference on Quantum electronics and Laser Science Conference, Baltimore, MD, USA, 2–4 June 2009.

**How to cite this article:** Mishra A, Noppari P, Boussard-Plédel C, Petit L, Massera J. Changes in the mechanical properties of bioactive borophosphate fiber when immersed in aqueous solutions. *Int J Appl Glass Sci*. 2020;00:1–10. <https://doi.org/10.1111/ijag.15514>